

Hybrid fuel cell-supercapacitor system: modeling and energy management using Proteus

Mohamed Haidoury¹, Mohammed Rachidi¹, Hicham El Hadraoui², Oussama Laayati²,
Zakaria Kourab³, Souad Tayane³, Mohamed Ennaji³

¹Modeling, Information Processing and Control Systems, National School of Arts and Crafts, Moulay Ismail University, Meknes, Morocco

²Green Tech Institute, Mohammed VI Polytechnic University, Benguerir, Morocco

³Laboratory Complex Cyber Physical Systems, National School of Arts and Crafts, Hassan II University, Casablanca, Morocco

Article Info

Article history:

Received May 11, 2023

Revised Aug 6, 2023

Accepted Oct 9, 2023

Keywords:

Energy management strategy

Equivalent circuit

Fuel cell

Hybrid system

Proteus

ABSTRACT

The increasing adoption of electric vehicles (EVs) presents a promising solution for achieving sustainable transportation and reducing carbon emissions. To keep pace with technological advancements in the vehicular industry, this paper proposes the development of a hybrid energy storage system (HESS) and an energy management strategy (EMS) for EVs, implemented using Proteus Spice Ver 8. The HESS consists of a proton exchange membrane fuel cell (PEMFC) as the primary source and a supercapacitor (SC) as the secondary source. The EMS, integrated into an electronic board based on the STM32, utilizes a low-pass filter algorithm to distribute energy between the sources. The accuracy of the proposed PEMFC and SC models is validated by comparing Proteus simulation results with experimental tests conducted on the Bahia didactic bench and Maxwell SC bench, respectively. To optimize energy efficiency, simulations of the HESS system involve adjusting the hybridization rate through changes in the cutoff frequency. The analysis compares the state-of-charge (SOC) of the SC and the voltage efficiency of the fuel cell (FC), across different frequencies to optimize overall system performance. The results highlight that the chosen strategy satisfies the energy demand while preserving the FC's dynamic performance and optimizing its utilization to the maximum.

This is an open access article under the [CC BY-SA](https://creativecommons.org/licenses/by-sa/4.0/) license.



Corresponding Author:

Mohamed Haidoury

Modeling, Information Processing and Control Systems, National School of Arts and Crafts, Moulay Ismail University

Meknes, Morocco

Email: haidoury.mohamed@gmail.com

1. INTRODUCTION

Global warming, the depletion of petroleum resources, the deterioration of air quality, and many inquiries into a pollution-free, healthy, and clean environment have heightened scientists' interest in developing alternative, sustainable and ecologically clean solutions in recent decades. In emerging economies, particularly in big cities, the transportation industry is a major source of toxic exhaust emissions into the environment, such as sulfur dioxide (SO₂), nitrogen oxides (NOX) and carbon monoxide (CO), posing a serious threat to life on our planet. The electrification of vehicle powertrains is commonly regarded as one of the most promising technologies in the automotive sector for increasing fuel economy (energy efficiency) and lowering greenhouse gas emissions [1]. The electric vehicle (EV) architecture refers to the location of the energy storage system and the components of the electric powertrain. This architecture is

more flexible than a conventional internal combustion engine (ICE) vehicle's architecture due to the reduction of the moving parts; the clutch and the conventional transmission system are replaced by a basic gear ratio, in addition to the simplification of the engine system. An EV is a system that could use a unique energy source or a hybrid energy storage system (HESS) that combines energy from multiple sources of different natures taking into consideration the characteristics of each source. The most common energy sources in an EV are usually the battery, fuel cell (FC) and supercapacitor (SC), besides photovoltaic panels that are still used in noncommercial and limited editions of electric vehicles [2].

Recently, many research works have been carried out on the topologies and energy management techniques among the HESS system's sources. The various topologies and combinations of energy sources, proposed by researchers, aim to design an efficient, reliable and economical system for an EV [3]. The most contemporary combination includes the FC-battery-SC, the FC-battery, the battery-SC, the FC-SC and the photovoltaic panels-Battery "e.g., Tesla Model 3, Honda Clarity and Lightyear One". The HESS system for EVs consists of a primary energy source and a secondary source [4], [5]. The main energy source ensures a long range, while the secondary energy source complements the main source during regenerative braking and acceleration and improves the performance of the system in terms of cost, lifetime and overall system efficiency [6], [7]. Currently, most EVs use the battery or FC as a primary source. Unlike the battery that stores energy for later use, the FC generates energy from hydrogen and oxygen. Therefore, battery technology remains limited given its low energy density, high cost, and the need for periodic replacement. For this reason, the FC is used as a main source, due to its high current density, ensuring an extended autonomy. However, it is constrained by its high cost and its low power density [8]. To balance the load demanded by the EV, an SC (with or without batteries) can be used as a secondary electrical source [9]–[11], contributing to tasks such as starting, acceleration, handling excessive energy demand and to recovering energy during regenerative braking. Since SCs are energy storage systems, they can be instantly charged and discharged. Many studies have been carried out regarding the modeling and simulation of the HESS systems [12], [13], with a focus on dimensioning of the primary and secondary electrical sources to extend their lifespan, reduce sources degradation and minimize the overall system cost [14], [15]; in addition to the validation of the architecture and topology of the designed HESS system, through the coupling between the source and the load using direct current to direct current converters (DC-DC) [11], [16]; and finally to develop an effective energy management strategy (EMS) that maximizes autonomy through efficient EMS [17], [18].

This paper aims to develop a model of the FC and SC within the Proteus environment. The developed models are validated by comparing the simulation results to the experimental data collected using the Bahia bench and a Maxwell SC module. On the other hand, the purpose is to design a HESS system based on the FC and SC under the Proteus environment. The EMS of the system realized by an algorithm based on a low-pass filter and implemented in an STM32 microcontroller.

The first section provides a literature review of the architecture of hybrid electric vehicles fuel cells (HEVFC) and analyzes several works regarding fuel cell and energy storage system development. The second section is dedicated to the development of models for the FC and SC source, as well as the HESS system of an EV using Proteus. The third section is devoted to the hardware used to validate the FC and SC model. The fourth section presents the simulation results of the model developed using the European driving cycle (ECE-15). And finally, conclusions are subsequently made to represent the comparisons and suggestions for future work.

2. STATE OF ART

In vehicles utilizing a FC as the primary source and a SC as an auxiliary source, the FC serves to provide extended range. Conversely, the SC functions to absorb energy during braking and to assist the FC during start-up, acceleration and peak demand periods, such as those required for electric vehicle loads (e.g., air conditioning, pilot lights) [19]. To ensure a consistent and dependable power supply to loads, suitable EMS are employed to regulate the various sources via DC-DC converters. In the relevant literature, three distinct topologies have been proposed for this purpose: series, cascade and parallel. Depending on how the loads are connected to the sources, three possible configurations exist [20]:

- A direct structure (zero degrees of freedom): which allows the sources to be connected directly to the load via the DC bus.
- An indirect structure with one converter (one of the degrees of freedom): which allows to associate a static converter to one of the two sources.
- A structure with two converters (two degrees of freedom): which consists in associating to each source a static converter.

In terms of practical implementation, the converter designed for the FC is unidirectional and commonly operates as a voltage boost converter. Conversely, the converter for the SC is bidirectional in power and typically a buck/boost converter, dependent on the mode of operation (energy recovery/supply). Regarding the EMS, numerous studies have investigated energy management techniques for distributing power between the primary source and secondary sources [21]. Among these techniques, rule-based algorithms such as low-pass filter-based energy distribution [22], [23], energy allocation by state-of-charge (SOC) of sources [24], [25], fuzzy logic [26], based on the slope of the road [27] and by optimization through a multi objective function [28]. The main disadvantage of this type is the lack of adaptability to different operating conditions: the control parameters will therefore not be optimal afterward. In addition, other energy management strategies have been studied based on optimization, such as the real-time optimal EMS. This one is based on the predictive control of the model [17], [29], other types of strategies are based on learning [30], [31]. Figure 1 illustrates various classifications of EMSs for EVs.

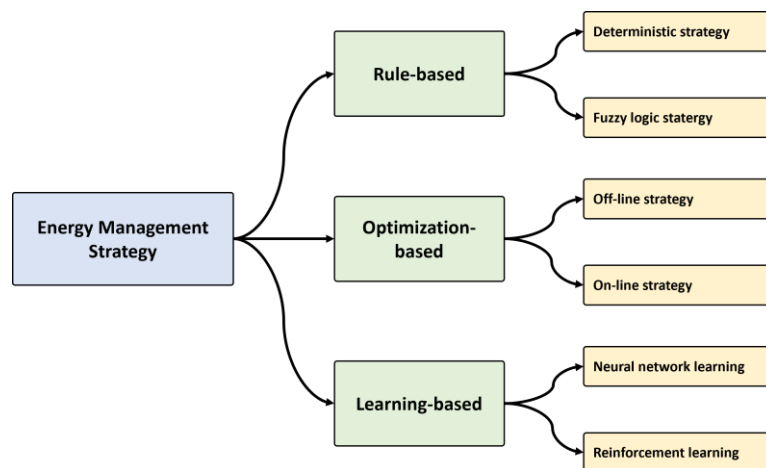


Figure 1. EMS classification of Evs

As a result, several other techniques are based on learning to achieve optimal control. They use a set of historical and real-time data to train the parameters of the strategy. These techniques are used to control the converters connected to energy sources. To assess the effectiveness of these methods, it is essential to test them before implementation. For this reason, researchers often use simulation tools such as Simscape, LTspice, and Advisor [32], [33]. Otherwise, MATLAB/Simulink remains the most popular simulation environment [34]–[36]. However, the main drawback of these tools is the lack of microcontrollers or embedded boards such as photonic integrated circuit (PIC), field-programmable gate array (FPGA), Arduino and STM32, which are essential for implementation and testing in real prototypes of the EMS power management algorithm, showing some limitations. On the other hand, the MATLAB/Simulink software integrates a MATLAB Coder tool that allows to export an algorithm in “C” code and compile it with an appropriate compiler. However, it is still limited by the size of the file converted by MATLAB Coder which remains huge compared to the code generated by the integrated development environment (IDE). In addition, MATLAB allocates dynamic memory for variables, which does not allow the definition of the variable type [37]. Moreover, this tool does not take into consideration the resources available on a microcontroller to execute the code (such as RAM). It should be noted that MATLAB is efficient for model validation and algorithm development, but when it comes to reimplementation from scratch so that they run efficiently on the microcontroller, additional considerations are required. Moreover, the sensors used in these discussed simulation tools are modeled as ideal components. However, using the Proteus tool can circumvent these problems since it is currently (as of 2020) the only electronic CAD tool that allows the design of a complete electronic system and its simulation, including the microcontroller code. To do so, it includes three modules:

- Visual designer is a diagram capture module or diagram editor (ISIS) that allows to design, test and debug whole embedded systems within the diagram capture before ordering a physical prototype.
- The simulation module “PROSPICE VSM” is an extension to the PROSPICE simulator that facilitates co-simulation.
- ARES is a placement-routage module that allows for the design, simulation, testing and quick production of professional printed circuit boards (PCBs).

Proteus is a versatile software that offers a range of features beyond its core modules. One notable functionality is the “IoT Builder”, which streamlines the development and deployment of internet of things (IoT) projects from design to implementation. Additionally, Proteus includes a microcontroller development environment complete with an algorithmic programming module. Its extensive libraries cater to various microcontrollers, such as PIC, Atmel ARM, and Cortex A0/A3/A4 [38]. Proteus also facilitates the integration of code developed in a specific IDE for microcontrollers by downloading the hexadecimal code, effectively mimicking the real upload process. With these comprehensive capabilities, Proteus serves as a valuable tool for diverse electronic design and development projects, empowering users to create innovative solutions across multiple domains.

Figure 2 illustrates the development steps under Proteus compared with those under MATLAB/Simulink. The development process with Proteus VSM is shown in Figure 2(a), while the development process with MATLAB/Simulink is represented in Figure 2(b). Comparing the two processes, Proteus allows the acceleration of the development time of an electronic board such as the EMS since the software development intervenes as soon as the schematic is drawn, allowing testing the interaction between the hardware and the software before the physical prototyping, whereas this is not feasible on MATLAB/Simulink. In addition, while the algorithm code implemented in the microcontroller on Proteus can be used directly in the real experiment, when using MATLAB/Simulink, the algorithm code must be redeveloped on specific compilers to be used on the microcontroller. For these reasons, researchers and engineers could take advantage of Proteus software to test and evaluate the performance of their algorithm before the actual implementation. However, the literature has not covered the simulation of a complete HESS system for EVs under the Proteus software, since the Proteus software does not support the FC and SC model; although recently, some works have focused on simulating photovoltaic (PV) panels in Proteus to test the maximum power point tracking MPPT [38], [39]. In this context, the main objective of this paper is to present a model of a HESS system. This model contains representations of both the FC and SC developed based on an equivalent electric circuit, a model of the EV load deduced from an ECE-15 driving cycle, vehicle characteristics developed based on easy VHDL hardware description language (VHDL), DC-DC converters, voltage and current sensors, and an EMS which was realized by an algorithm based on a low-pass filter and implemented in an STM32 microcontroller. The remaining sections of this paper elaborate on the design aspects of the HESS system under Proteus.

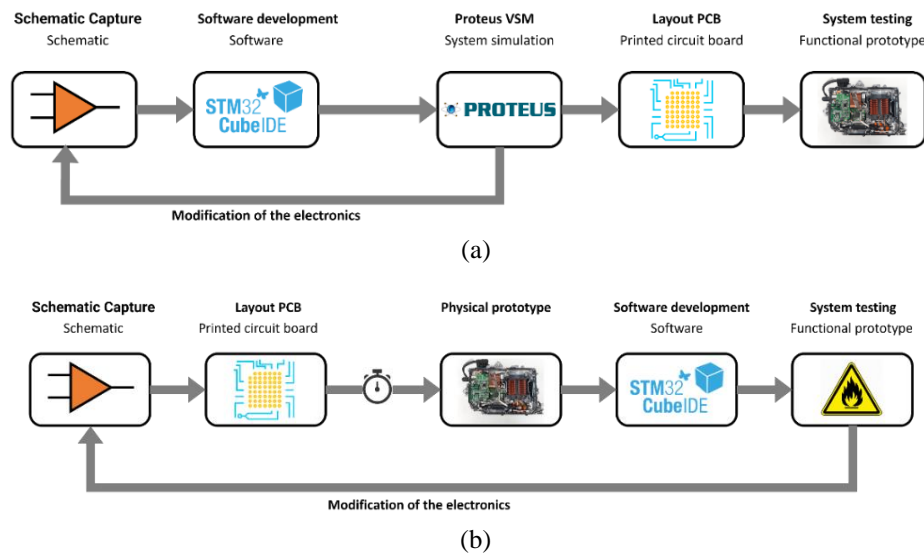


Figure 2. Design process comparison (a) with Proteus VSM and (b) without Proteus VSM

3. HYBRID ESS MODEL

Figure 3 illustrates the architecture employed in the development of the HESS under Proteus. This HESS system includes a primary source consisting of a proton exchange membrane fuel cell (PEMFC) coupled with a DC/DC boost converter. Additionally, a secondary source incorporating a SC is included, which enables the production and absorption of high powers, this source is connected to a bidirectional DC/DC converter. These two sources are connected to the load through a capacitor [16]. The control of both converters is managed by an EMS that facilitates efficient energy management.

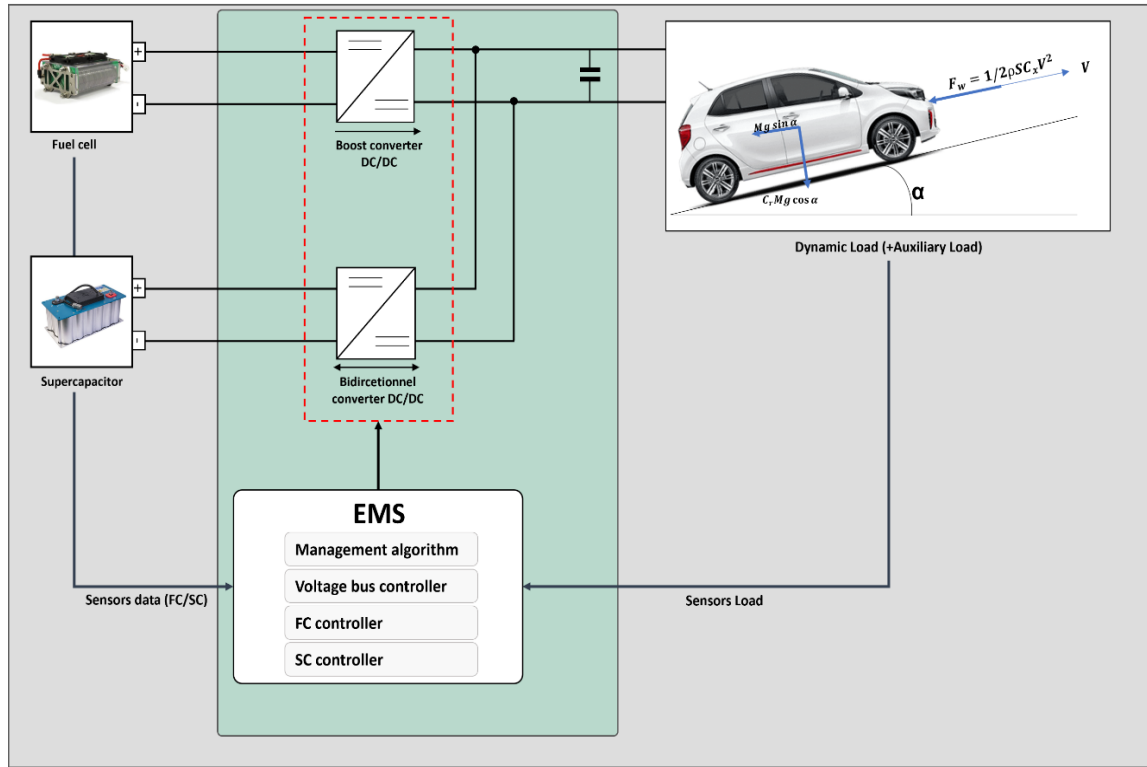


Figure 3. HESS architecture utilized for the model developed under Proteus

3.1. PEMFC model

The FC system is an electrochemical device that converts chemical energy into electrical energy through a reaction of oxidation-reduction. This process involves the reaction of hydrogen with oxygen, as represented by (1), producing water, heat and electrical power. The FC system is modeled by a complex system that enables it to generate its dynamic behavior by modeling various phenomena, including energy losses, double layer capacity, and the chemical delay due to the hydrogen and oxygen chemical reaction. Alternatively, there are models based on energy representations such as the Bond graph (BG) and energetic macroscopic representation (EMR) [34], [35], and models based on neural networks [40], [41]. However, the disadvantage of these models is the fact that they require a longer computation time. For this purpose, simplified models based on equivalent electrical circuits, as illustrated in Figure 4, were employed in this study [42]. *RC*-type models are shown in Figure 4(a), while *RL*-type models are shown in Figure 4(b). These models allow representing a static behavior identical to that of non-linear FC models and provide good transient behavior. The equivalent electrical circuit used to develop the model in Proteus is of the *RC* type.



The equivalent circuit of the FC is depicted in Figure 4, consisting of a voltage source E_n , a shunt resistor (R_m or R_1), a series resistor (R_t or R_2), and either a capacitor C or an inductor L . The voltage produced by the PEMFC can be calculated using Nernst voltage and is represented by the (2)-(4) [42], [43].

$$E_0 = 1.4648 - 4.510 \cdot 10^{-4}T + 1.025610 \cdot 10^{-8}T^2 + 9.5210 \cdot 10^{-13}T^3 - 5.98910 \cdot 10^{-5}T \ln(T) \quad (2)$$

$$\Delta E = (R \cdot T_{fc} / N_e \cdot F) \ln(P_{sc_{H_2}} / P_0) + (R \cdot T_{fc} / 2 \cdot N_e \cdot F) \ln(P_{sc_{O_2}} / P_0) \quad (3)$$

$$E_{nerst} = E_n + \Delta E \quad (4)$$

When the PEMFC delivers current, the Nernst potential decreases due to potential losses as described in (5) and (6) [43]. The final potential delivered by the FC, denoted as E_{fc} , can be determined using (7), while the specific parameters are listed in Table 1.

$$E_{act} = -0.848 + T \cdot \left(2.8610^{-3} + 0.210^{-4} \cdot \ln(A) + 4.310^{-5} \ln \left(\frac{PH}{1.0910^6 \cdot \exp\left(\frac{77}{T}\right)} \right) + 7.810^{-5} \cdot \ln \left(\frac{PO}{5.0810^6 \cdot \exp\left(-\frac{498}{T}\right)} \right) \right) \tag{5}$$

$$E_{ohm} = R_m I_{fc} \tag{6}$$

$$E_{fc} = N_c (E_n + \Delta E - E_{act}) \tag{7}$$

The FC exhibits a capacitive impedance, which arises from the ionic and electronic charge transfer phenomena occurring at the diffusion layers and electrode/electrolyte interface. To model this capacitive impedance in a PEMFC, an equivalent circuit (Rt//C) is commonly employed. To establish the model of the FC using the Proteus tool, an equivalent electrical circuit was realized with a voltage source parameterized using a Spice script according to the FC characteristics. Figure 5 illustrates the sub-circuit diagram of the model presented in Proteus software alongside its corresponding Spice code. The various parameters of the sub-circuit diagram for the Proteus FC are listed in Table 2.

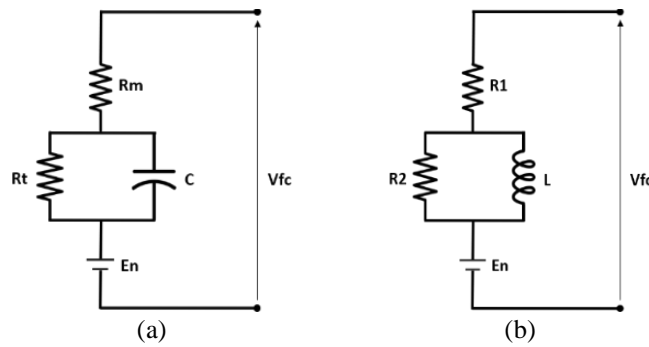


Figure 4. Equivalent electrical circuit of FC (a) RC type and (b) RL type

Table 1. Various parameters of the Nernst equation

Parameters	Value
Faraday constant	$F = 96485 \text{ C/mol}$
Perfect gas constant	$R = 8.3144621 \text{ J/mol/K}$
Operating temperature	$T0 = 298.15 \text{ K}$
Atmospheric pressure	$P0 = 101325 \text{ Pa}$
Active exchange surface	$A = 100 \text{ cm}^2$
Number of electrons exchanged	$Ne = 2$
Number of stacks	$Nc = 24$

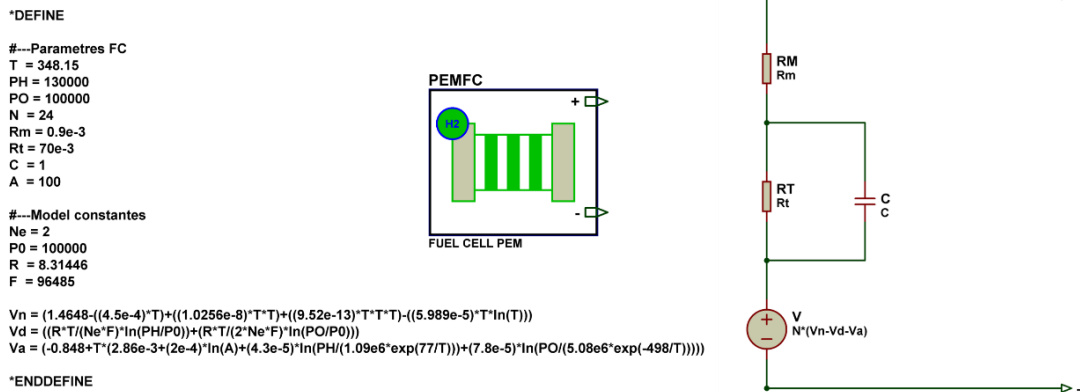


Figure 5. Circuit diagram of the proposed FC model under Proteus

Table 2. Various parameters of the FC model in Proteus

Parameters	Value
Operating temperature	$T = 348.15 K$
Pressure oxygen	$PO = 100000 Pa$
Pressure hydrogen	$PH = 130000 Pa$
Charge transfer capacitor	$C = 5 F$
Charge transfer resistance	$Rt = 70e^{-3} \Omega$
Ohmic resistance	$Rm = 0.9e^{-3} \Omega$
Number of cellules	$N = 24$

3.2. Supercapacitor model

The SC is an electrochemical capacitor with high energy density. It allows the storage of electrical energy with a higher energy density and restores it quickly. Due to this characteristic, it is used in electric traction applications, to provide the power required in transient conditions. Several works are carried out on the modeling of SCs. Among these models, there are dynamic energy models, which consider the partition of the electrostatic energy of the SCs into two energies, one quickly stored and the other slowly stored [44]. Other models of SCs are simplified models based on RC circuit given by the (8) [45]. This model is based on an ideal capacitor representing the equivalent capacitance of the supercapacitor, to which a series-connected resistor represents the equivalent resistance of the supercapacitor. The Figure 6 illustrates the equivalent circuit model of the SC, and the corresponding model parameters can be found in Table 3. The SOC of the SC is calculated using a code programmed under STM32, enabling the deduction of its value from (9).

$$V_{SC} = R_{SC}I_{SC} + \frac{1}{C_{SC}} \int I_{SC} dt \quad (8)$$

$$SOC_{SC} = (SOC_{SC}(t_0) - \frac{1}{C_{SC}V_{max\ sc}} \int I_{SC} dt) \times 100 \quad (9)$$

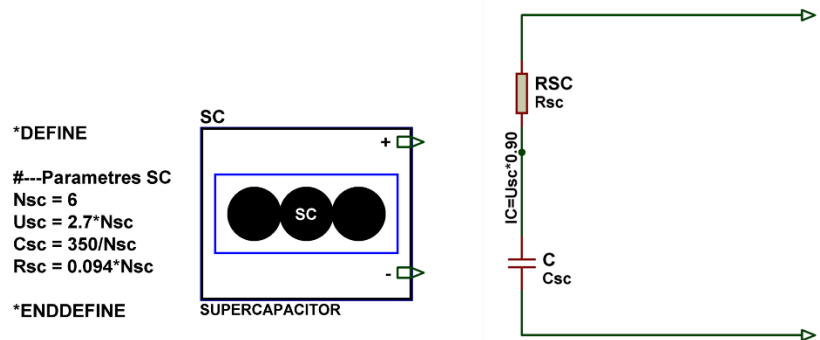


Figure 6. Proposed SC model circuit diagram in Proteus

Table 3. The different parameters of model SC Proteus

Parameters	Value
Equivalent Resistance	$R_{sc} = 0.3 \Omega$
Equivalent Capacity	$C_{sc} = 300 F$
Voltage	$V_{sc} = 16 V$
Number of cells	6 in series

3.3. Load model

The validation of the developed HESS system must be performed using a power profile requested by the load. This load profile is deduced from the urban driving cycle ECE-15 and the mechanical characteristics of the EV. This driving cycle has been decomposed into several linear segments over specific time intervals. This decomposition into linear segments enables the velocity profile to be represented as a function defined by parts in partial periods, as shown in Figure 7. Thus, the velocity equation $V(t)$ for a segment passing through points (t_i, V_i) and (t_{i+1}, V_{i+1}) is given by (10).

$$V(t) = \frac{V_{i+1}-V_i}{t_{i+1}-t_i} \cdot t + (V_i - \frac{V_{i+1}-V_i}{t_{i+1}-t_i} \cdot t_i) \tag{10}$$

The calculated power profile is adjusted by scaling it to 1/200 to match the available power on the bench. Subsequently, this profile is divided by the bus voltage to determine the required current. It is then modeled by a ‘‘Current Source’’ block implemented in easy VHDL using (11). The parameters of the equation in question are shown in Table 4 and the current required by the load is illustrated in Figure 8.

$$P_m = V(M \cdot g \cdot \sin \alpha + C_r \cdot M \cdot g \cdot \cos \alpha + \frac{M \cdot dV}{dt} + \frac{1}{2} \rho \cdot S \cdot C_x \cdot V^2) \tag{11}$$

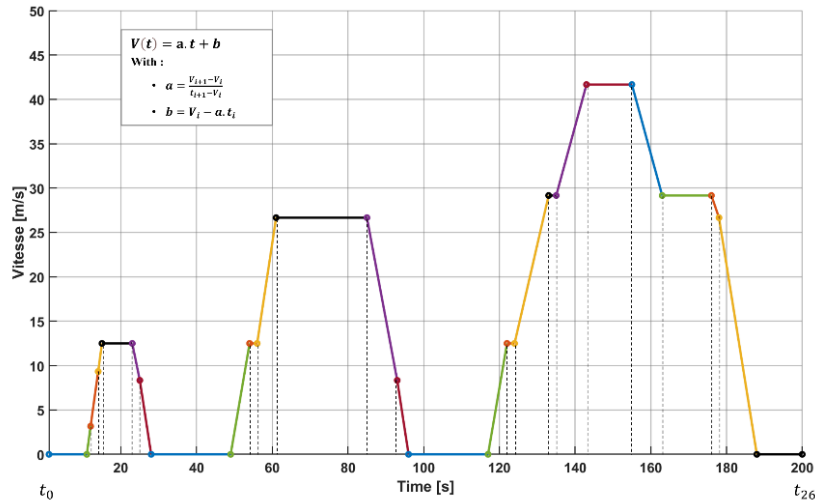


Figure 7. The ECE-15 urban driving cycle represented by a function defined on intervals

Table 4. The different parameters of VE

Parameters	Value
Vehicle speed	ECE-15 cycle (m/s)
Road Grade	0 %
Coefficient of rolling resistance	0.02
Aerodynamic coefficient	0.70
Gravitational constant	9.81 m/s ²
Air density	1.255 Kg/m ³
Vehicle mass	1450 Kg
Front surface	2.5 m ²

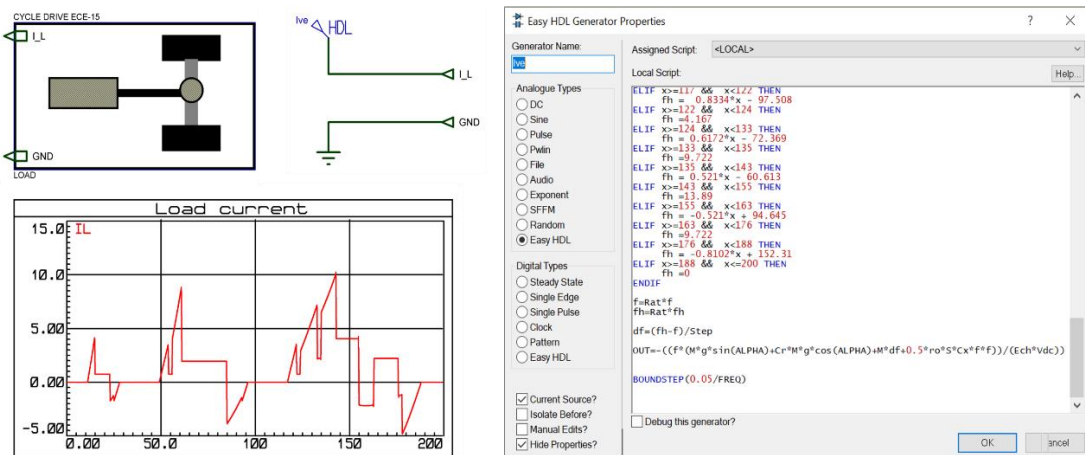


Figure 8. Circuit diagram of the proposed load model under Proteus

3.4. Control strategy

The HESS system's energy demand is achieved by the reallocation of energy between the different sources of the system through an appropriate EMS, respecting the characteristics of each source. The strategy used in this article is the frequency decomposition of the power demand. A low-pass filter is used with a cutoff frequency $f_0 = 0.2 \text{ Hz}$ [35], [46]. The algorithm, implemented in an STM32 microcontroller and shown in Figure 9, was developed based on these objectives. The configuration and I/O of the STM32 is given in Table 5. The aims of this strategy are the following: i) meet the EV's power demand, ii) maintain constant bus voltage, iii) respect the slow dynamics of the FC, iv) recover and store kinetic energy during braking on the SC, and v) monitor and maintain the SOC of the SC in its optimal range between 60% and 100%.

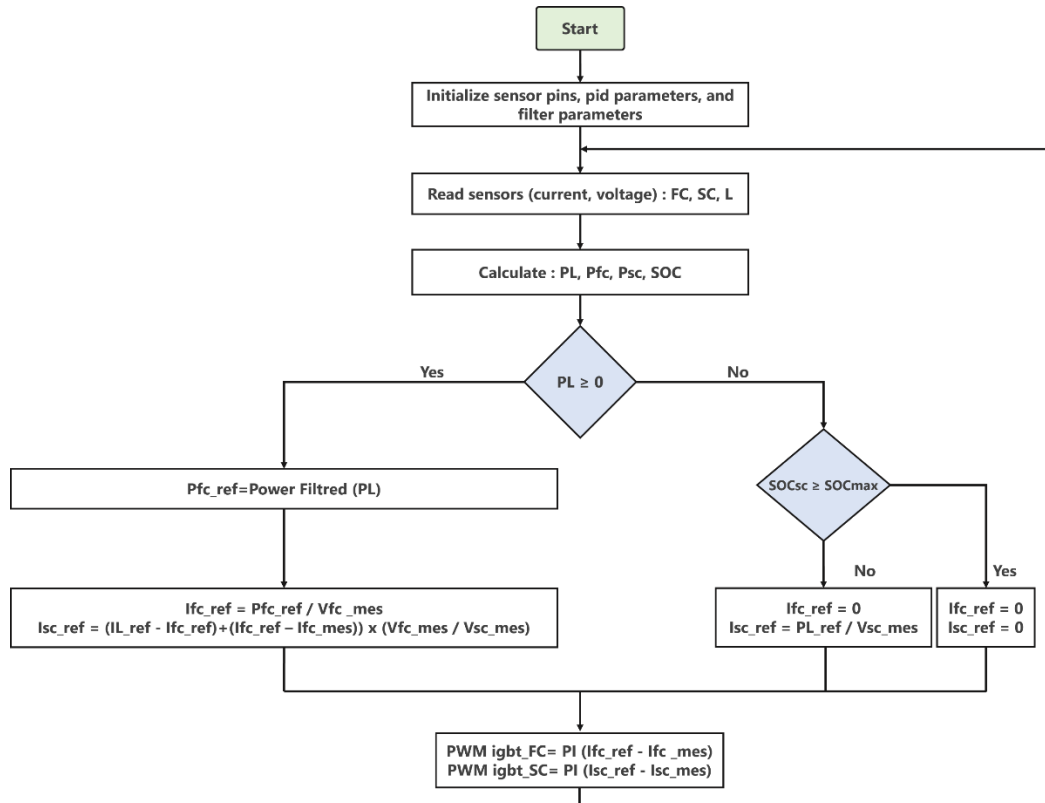


Figure 9. EMS algorithm

Table 5. The different parameters of STM32

Configuration	Value
Clock frequency	72 MHz
Timer 1 (Generate a PWM signal on output pin PA9, PA10 and PA11)	10 KHz
Timer 2 (generate an interrupt every 0.01 ms)	100 KHz
ADC1 (Analog input used to measure a voltage and current from FC, SC and Load)	IN0-IN5
UART1 (Used for serial communication PB6 and PB7)	115200

3.5. The whole HESS system

The HESS developed in Proteus contains several blocks, which enable the representation of the load, various sources and converters as follows: i) a load block developed that enables requesting power similar to that of an EV; ii) a developed FC block that can deliver power according to these characteristics programmed in the Spice code; iii) an SC block is developed to provide power according to these characteristics programmed in the Spice code; iv) a step-up converter block developed based on an insulated-gate bipolar transistor (IGBT), this block is connected to the FC [47]; v) a bidirectional converter block developed based on two IGBTs. It is connected to the SC [48]; vi) a coupling capacitor enables the coupling of the load with the two FC/SC sources.

The EMS developed in Proteus requires certain measurements, namely the power demanded by the load and the powers supplied by the sources. The components used for the development of the EMS in the Proteus tool are the following:

- Three sensor blocks, each block contains a current sensor and a voltage sensor. These blocks measure the current and voltage required by the load and the currents and voltages supplied by the sources.
- An EMS block based on an STM32 microcontroller that allows the management of the re-distribution of the energy between the sources and supervises them through the measured parameters: current, voltage and power.

In addition to the developed simulator, a serial port integration has been incorporated into the system to facilitate the monitoring of energy generation from the FC and the SC, as well as the energy demand from the load. This serial port enables real-time data acquisition and communication between the HESS system and external devices. Figure 10 visually presents the implementation of the HESS within a VE as realized under Proteus.

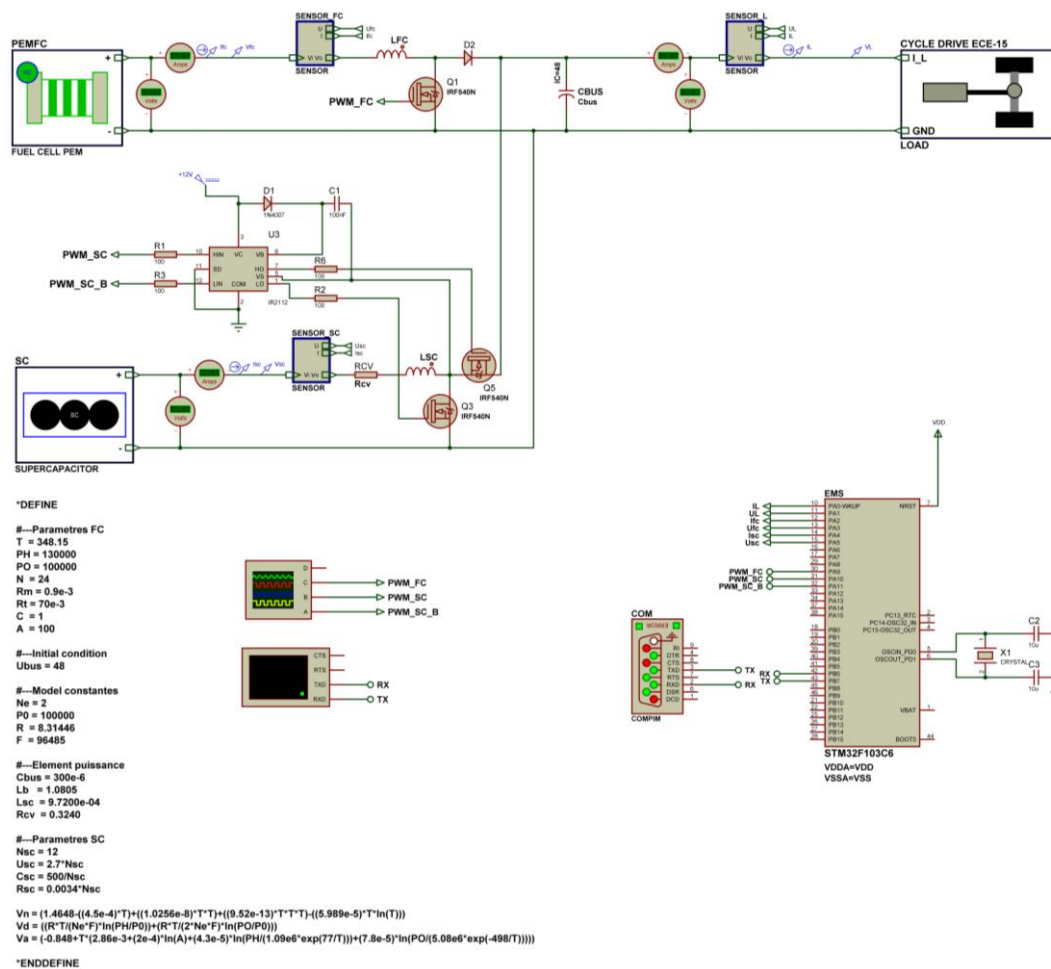


Figure 10. Components of the proposed HESS model in Proteus software

4. MATERIALS AND METHODS

The FC model developed in Proteus was experimentally validated using the Bahia bench by comparing the dynamic behavior of the developed model with the experimental results of the bench. This platform is equipped with 24 PEMFC cells, with a maximum power of 1.2 kW and a nominal current of 65 A, along with an output voltage ranging from 14 to 22 V. The Bahia bench is equipped with a human machine interface (HMI) that allows configuring the load current and retrieving the voltage provided by the FC, in order to compare it with the results of the proposed model, as illustrated in Figure 11.

The SC model was validated with a Maxwell SC bank consisting of six SCs connected in series. The comparison between the charging and discharging behavior of the Maxwell SC module and the model

developed under Proteus is shown in Figure 12. Experimental data gathered from the PEMFC Bahia test bench and the Maxwell SC module serve as the basis for validating the FC and SC modules, respectively, both of which have been developed using Proteus software. This comprehensive validation process ensures the accuracy and reliability of the proposed models, providing a solid foundation for the HESS and EMS in EVs.

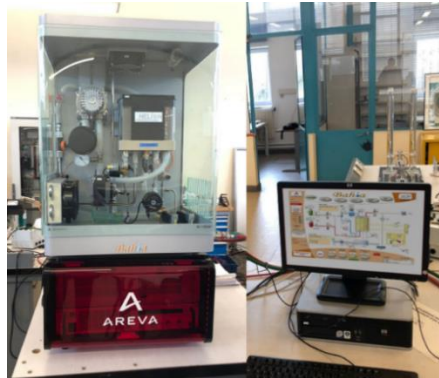


Figure 11. The PEMFC Bahia test bench



Figure 12. Setup for charge and discharge tests of the SC module

5. RESULTS AND DISCUSSION

In order to validate the HESS system simulator developed under Proteus, the first step involves validating the performance of the energy sources. For the FC, this includes comparing the dynamic and static behavior of the model with experimental results. Similarly, for the SC, the charge and discharge of the module are compared with the results obtained from the test bench. Subsequently, the second stage of validation encompasses assessing the overall performance of the HESS system. This evaluation focuses on verifying the system's effectiveness and functionality as an integrated entity.

5.1. Validation of the FC model

With the aim of evaluating the PEMFC model developed under Proteus, it is therefore, necessary to compare the dynamic and static behavior of the proposed model with the experimental data of the Bahia bench. For this purpose, we obtained the voltage and current readings delivered by the Bahia bench at a temperature $T_{fc} = 75\text{ }^{\circ}\text{C}$ and a stoichiometry value $C_{sto\sigma_{O_2}} = 2$. The measured data were contrasted with the proposed Proteus model. Considering the experimental results obtained from the Bahia bench in comparison with its dynamic and static behavior, the PEMFC model proposed in Proteus was validated, as evidenced by its consistent performance in both transient and steady states, due to the double layer capacity and the ohmic losses of the PEMFC. The static behavior is defined for a typical ramp current profile of 0-60 A. Figure 13 shows the bias curves of the FC model, compared to the experimental results. To evaluate the model, we calculated the root mean square error (RMSE) of the model developed in Proteus compared to the experimental data, resulting in a value of 0.27139. In a steady state, the error is minimal, and the model is capable of accurately predicting the ohmic resistance phenomenon.

The dynamic behavior is defined for a typical pulse current profile from 20 to 60 A. Figure 14 shows the output voltage of the Bahia bench in comparison with the output voltage of the developed model. According to this figure, the proposed model under Proteus exhibits a dynamic characteristic during the temporary transient phase, enabling the prediction of the transitions due to the effect of the double layer capacitor.

5.2. Validation of the SC model

The SC model was validated by comparing the experimental result of the Maxwell SC bank with the model developed under Proteus, during the charge and discharge of the SC. Figure 15 illustrates a comprehensive comparison between the setpoint and the response generated by the model. The load response, as depicted in Figure 15(a), and the discharge response, as portrayed in Figure 15(b), are presented side by side. Notably, a striking similarity is observed between the responses obtained from the model developed within the Proteus framework and the corresponding experimental results. The degree of resemblance between the two sets of responses is remarkably high.

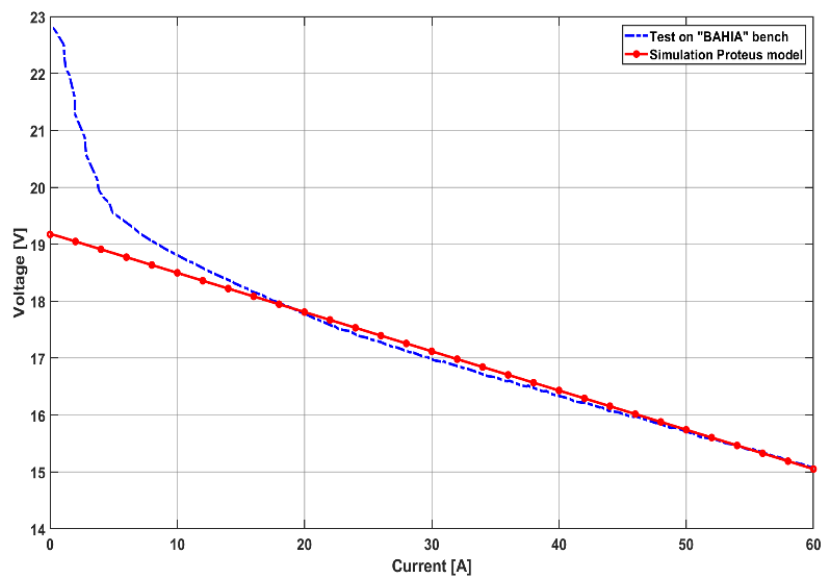


Figure 13. Comparison of model and experimental polarization curves

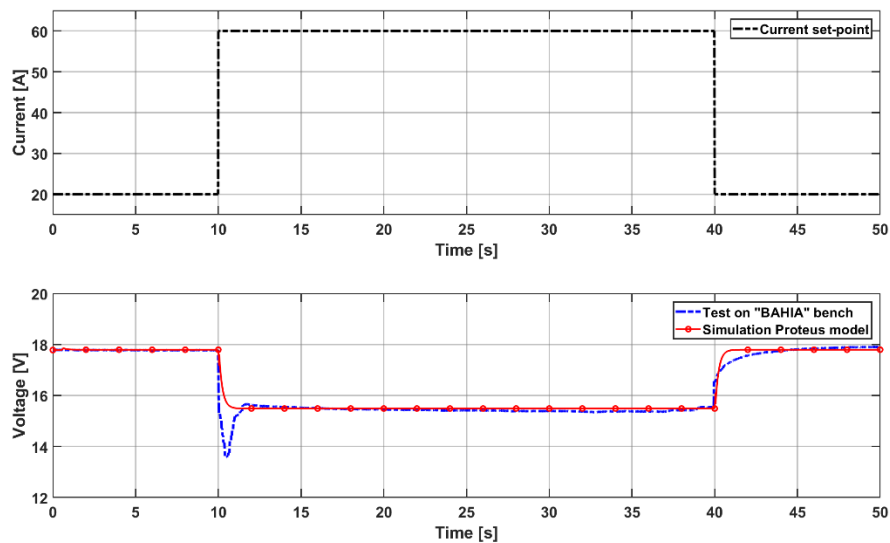


Figure 14. Response of various models to pulse current demand

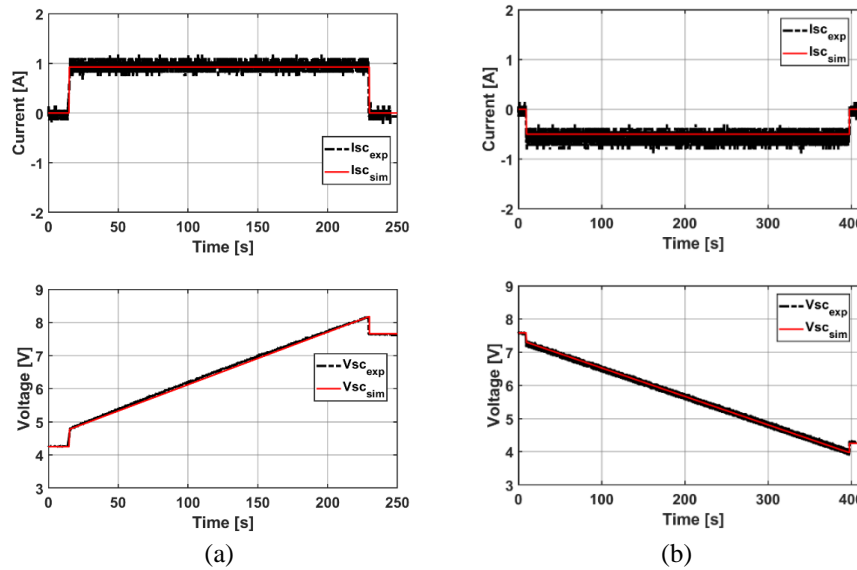


Figure 15. Demand and response of the supercapacitor (a) recovery and (b) delivery

5.3. Simulation of the HESS system and the EMS

The HESS system simulator, designed under Proteus, provides the power required for the load. This energy is calculated from the sensors installed on the system (current and voltage), then distributed through a 1st order “Butterworth” low-pass digital filter. This filter is developed in a library under STM32. The reference power that must be provided by the FC is calculated from the power requested by the load (positive part) by acting on the cutoff frequency, the rest of the power is provided by the SC. Figure 16 shows the power demanded by the load and the power to be supplied by the FC source for cut-off frequencies of 0.2, 0.1, 0.05, and 0.02 Hz. The simulation results show that the filter library designed under STM32 allows to distribute the power according to the real-time data measured on the sensors.

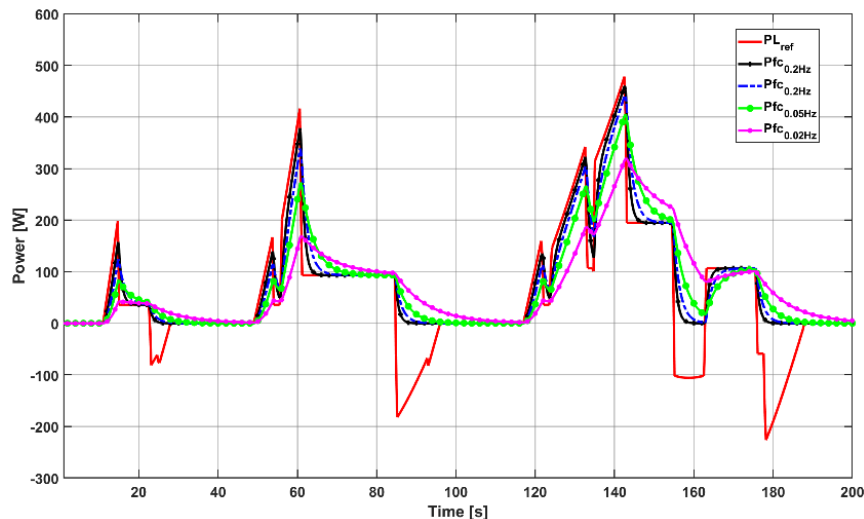


Figure 16. Comparison of the power distribution for different cut-off frequencies

The performance of the HESS system and the EMS was evaluated by the load profile deduced from the European ECE-15 driving cycle. The results obtained, as shown in Figure 17, illustrate that the bus voltage remains constant with minor fluctuations. The bus voltage is regulated with a digital PI at 48 V despite a fluctuating power demand of the load.

The variation in the state of charge as a function of the cut-off frequency is depicted in Figure 18 for multiple frequencies, namely, 0.2, 0.1, 0.05, and 0.02 Hz. These cut-off frequencies guarantee the maintenance of the SOC within the recommended range of 65% to 90%, thus ensuring optimal operation of the SC. However, when the frequency is lower than 0.02 Hz, the SOC falls outside of this range and may cause operational issues. Therefore, it is essential to select the cut-off frequency appropriately to optimize the power contribution from the SC and FC sources. To maximize the utilization of the FC, a maximum cut-off frequency of 0.2 Hz should be selected, while, to reduce the usage of the FC and maximize the contribution of the SC, a minimum cut-off frequency of 0.02 Hz is recommended. Figure 19 displays the electrical efficiency of the PEMFC as a function of the cut-off frequency. The results indicate that the electrical efficiency ranges are between 40% and 70%. During the acceleration phases of the ECE driving cycle (ascending), the electrical efficiency of the PEMFC increases as the cutoff frequency rises, particularly when the FC is used alone, achieving maximum efficiency. Conversely, during the deceleration phases of the ECE driving cycle (descending), the electrical efficiency decreases with the increasing cut-off frequency. These observations, along with those regarding the SOC, should be considered when defining a limiting cut-off frequency to ensure optimal operation of the PEMFC. Studies are ongoing to determine the optimal cut-off frequency for the PEMFC, considering auxiliary components of the FC, such as the air compressor. However, the primary focus of this paper is to develop a HESS simulator under Proteus for testing energy distribution algorithms and designing an EMS board. Therefore, a cut-off frequency of 0.1 Hz is used for the simulations in the remainder of the paper, without attempting to precisely define the optimal frequency considering the auxiliary components of the FC.

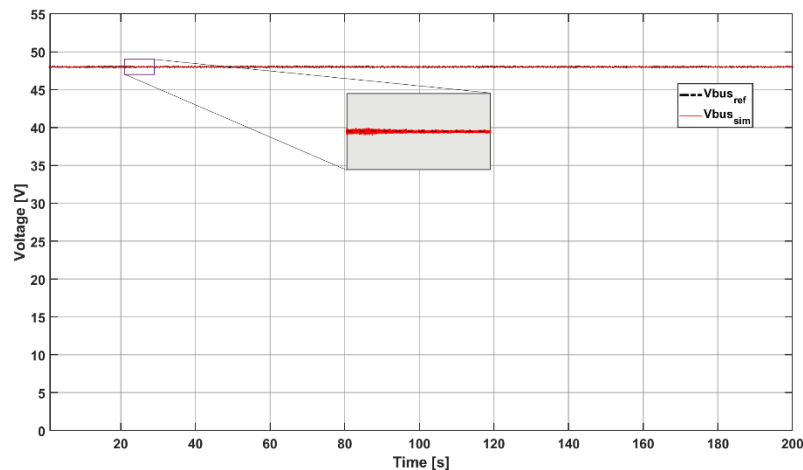


Figure 17. Bus voltage control

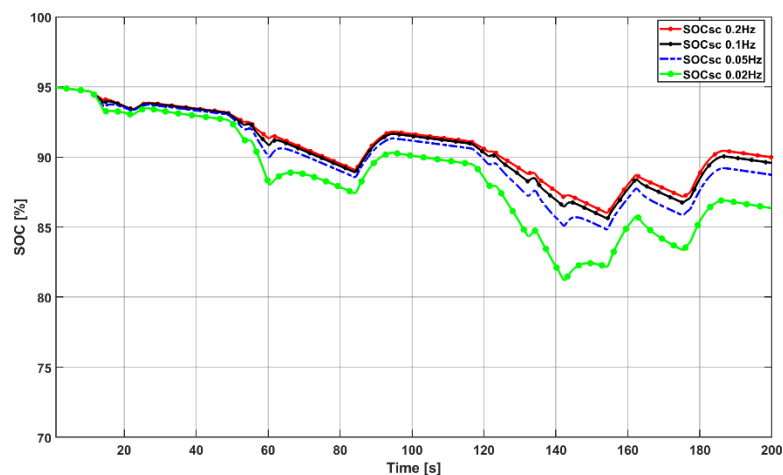


Figure 18. Comparison of the SOC SC for different cut-off frequencies

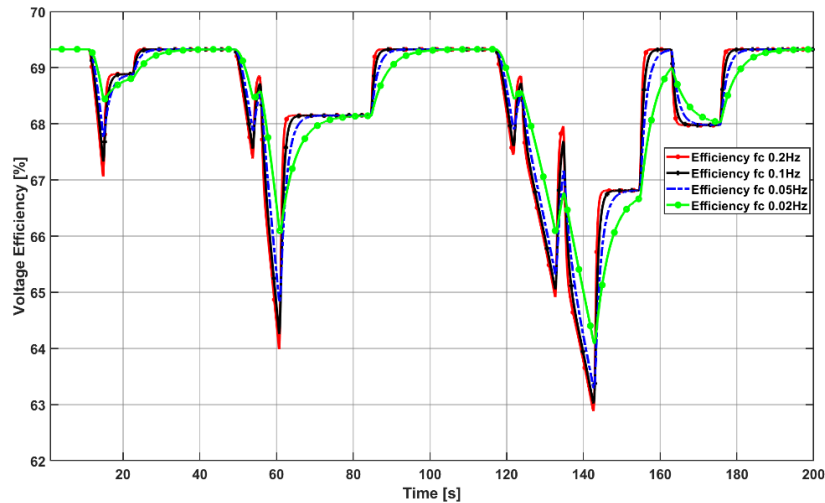


Figure 19. Comparison of the voltage efficiency for different cut-off frequencies

The simulation results of the HESS system have indeed allowed to verify the efficiency of the EMS based on a low-pass filtering with a cut-off frequency of 0.1 Hz and demonstrate the achievement of the objectives of the strategy. Undoubtedly, the total power demanded by the load during the urban driven cycle is provided without any problem. Moreover, these results additionally demonstrate that FC supplies energy during the permanent phases and provides the majority of the power demanded. This allows to respect its slow dynamics. On the other hand, the SC handles the energy demand in transient regimes. Figure 20, shows a comparison between the power demand (required) and the powers provided by the FC and SC sources, the results demonstrate that the strategy used ensures the maximum use of the FC, compared to the contribution of the SC.

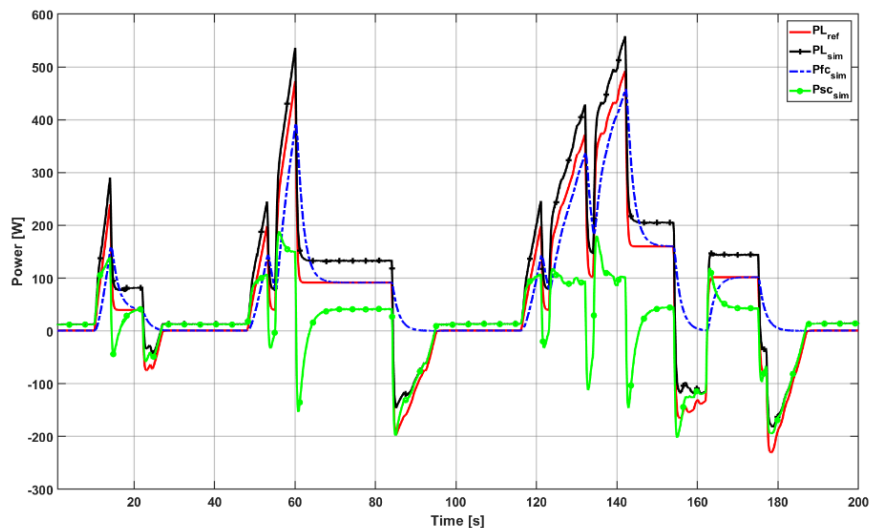


Figure 20. Comparison between the requested power (ECE-15) and the powers provided by the FC and SC

The output voltage of the SC must be maintained around 28.8 V, equivalent to 90% of its maximum load which is 32 V. The simulation results verified the energy recovery from the actuator to the SC during the deceleration and braking phases, which guaranteed that the SOC of the SC is maintained in the range [70%, 90%] throughout the simulation, ensuring the energy efficiency of the SC. The results also show that the SOC of the SC remains within the safe operating limits in the range [60%, 90%], which leads to higher utilization of the SC in transient regimes. Figure 21 shows the response of the FC and the SC.

The simulation results presented in this study demonstrate the effectiveness of the proposed HESS for electric vehicles. Firstly, the blocks of the FC and SC developed under Proteus are validated, and these models can be used as a library by modifying the characteristics of the SC and FC blocks in the Spice script. These blocks can be valuable for developing the DC/DC converters of each source while taking advantage of the Proteus tool which provides the capability to design electronic boards and simulate them prior to prototype realization. Secondly, the HESS system developed under Proteus has shown that the topology used, as well as the EMS developed under STM32, allows efficient energy management. Thus, the HESS system proposed under Proteus can be used either to validate other topologies or to design a new EMS. By using Proteus for the development and design of the prototype of HESS systems composed of an FC, a SC and/or a battery, it is possible to reduce the design time since it allows to simulate and validate an electronic design before the realization of a real prototype.

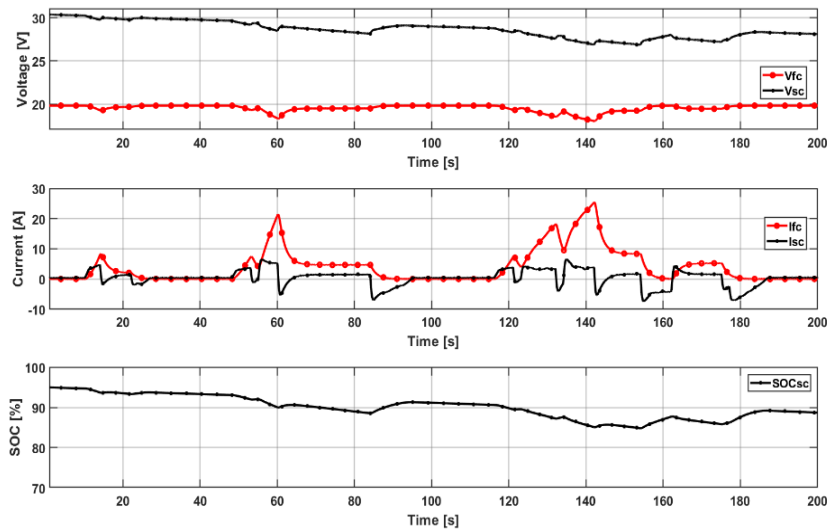


Figure 21. Voltage and current responses of FC and SC sources

6. CONCLUSION

A fuel cell hybrid electric vehicle (FCHEV) powertrain incorporates multiple power sources, each having distinctive energetic properties. This necessitates the careful design of an energy management system (EMS) to optimize the vehicle's performance in terms of fuel efficiency, longevity and durability. Although numerous EMSs have been developed for FCHEVs, most are based on static models that do not account for the variable operating conditions, aging and degradation phenomena that impact drivetrain components such as fuel cells, batteries and supercapacitors. Studies indicate that insufficient health adaptability could lead to a 6.5% to 24% increase in hydrogen consumption, depending on the EMS employed. Thus, it is imperative to focus on the design and modeling of accurate real-time systems and robust simulations, which are vital to fostering the development of more resilient and efficient systems.

The simulation results serve two main purposes: firstly, the fuel cell (FC) and supercapacitor (SC) blocks, developed and validated using Proteus, can be utilized as versatile library models with adjustable characteristics in the Spice script, facilitating the creation of customized DC/DC converters for each power source while leveraging Proteus for electronic board design and pre-prototyping simulation. Secondly, the HESS system, developed within the Proteus framework, demonstrates remarkable energy management efficiency, thanks to the chosen topology and the carefully designed EMS using STM32. Given this encouraging outcome, the proposed HESS system in Proteus holds the potential to validate alternative topologies or serve as a foundation for designing a novel EMS. Utilizing Proteus for developing and designing HESS prototypes, comprising an FC, SC and/or battery holds the potential to significantly reduce design time by simulating and validating electronic designs before constructing physical prototypes.

The Proteus-based simulator significantly contributes to the testing and simulating power electronic designs for HESS, as well as validating EMS algorithms. Once parameterized, this versatile simulator allows for direct microcontroller implementation, providing various testing and simulation possibilities before constructing a physical prototype. This streamlined approach facilitates efficient development and optimization of HESS and EMS designs.

Future research will focus on incorporating proton exchange membrane fuel cell (PEMFC) lifetime prediction methods into a C code library, which can then be integrated into an EMS. This approach will facilitate more effective control and management of PEMFC performance throughout its lifecycle. Additionally, further investigations will be conducted to expand the current understanding of PEMFC technology and explore new potential applications, driving innovation and advancements in the field of sustainable energy solutions for transportation.

REFERENCES

- [1] H. El Hadraoui, M. Zegrari, A. Chebak, O. Laayati, and N. Guennouni, "A multi-criteria analysis and trends of electric motors for electric vehicles," *World Electric Vehicle Journal*, vol. 13, no. 4, Apr. 2022, doi: 10.3390/wevj13040065.
- [2] S. Verma *et al.*, "A comprehensive review on energy storage in hybrid electric vehicle," *Journal of Traffic and Transportation Engineering (English Edition)*, vol. 8, no. 5, pp. 621–637, Oct. 2021, doi: 10.1016/j.jtte.2021.09.001.
- [3] C. H. Srinivas, V. H. Kumar, and T. A. Deepthi, "Simulation of hybrid electric energy storage system (HEES) for hybrid electric vehicle for power applications," *International Journal of Research*, vol. 9, no. 5, pp. 102–110, 2020.
- [4] S. M. Faresse, M. Assini, and A. Saad, "Hybrid energy storage system optimal sizing for urban electrical bus regarding battery thermal behavior," *International Journal of Electrical and Computer Engineering (IJECE)*, vol. 10, no. 3, pp. 2894–2911, Jun. 2020, doi: 10.11591/ijece.v10i3.pp2894-2911.
- [5] Z. Huang, C. Zhang, T. Zeng, C. Lv, and S. H. Chan, "Modeling and energy management of a photovoltaic-fuel cell-battery hybrid electric vehicle," *Energy Storage*, vol. 1, no. 3, Jun. 2019, doi: 10.1002/est2.61.
- [6] Y. Jiao and D. Månsson, "A study of the energy exchange within a hybrid energy storage system and a comparison of the capacities, lifetimes, and costs of different systems," *Energies*, vol. 14, no. 21, Oct. 2021, doi: 10.3390/en14217045.
- [7] J. Nájera, P. Moreno-Torres, M. Lafoz, R. de Castro, and J. R. Arribas, "Approach to hybrid energy storage systems dimensioning for urban electric buses regarding efficiency and battery aging," *Energies*, vol. 10, no. 11, Oct. 2017, doi: 10.3390/en10111708.
- [8] J. S. Artal-Sevil, J. L. Bernal-Agustín, R. Dufo-López, and J. A. Domínguez-Navarro, "Forklifts, automated guided vehicles and horizontal order pickers in industrial environments. energy management of an active hybrid power system based on batteries, PEM fuel cells and ultracapacitors," *Renewable Energy and Power Quality Journal*, vol. 1, no. 15, pp. 859–864, Apr. 2017, doi: 10.24084/repqj15.497.
- [9] H. Chen, Z. Zhang, C. Guan, and H. Gao, "Optimization of sizing and frequency control in battery/supercapacitor hybrid energy storage system for fuel cell ship," *Energy*, vol. 197, Apr. 2020, doi: 10.1016/j.energy.2020.117285.
- [10] V. Mounica and Y. P. Obulesu, "Hybrid power management strategy with fuel cell, battery, and supercapacitor for fuel economy in hybrid electric vehicle application," *Energies*, vol. 15, no. 12, Jun. 2022, doi: 10.3390/en15124185.
- [11] P. Yu, M. Li, Y. Wang, and Z. Chen, "Fuel cell hybrid electric vehicles: a review of topologies and energy management strategies," *World Electric Vehicle Journal*, vol. 13, no. 9, Sep. 2022, doi: 10.3390/wevj13090172.
- [12] M. İnci, M. Büyüç, M. H. Demir, and G. İlber, "A review and research on fuel cell electric vehicles: Topologies, power electronic converters, energy management methods, technical challenges, marketing and future aspects," *Renewable and Sustainable Energy Reviews*, vol. 137, Mar. 2021, doi: 10.1016/j.rser.2020.110648.
- [13] M. Kandidayeni, J. P. Trovão, M. Soleymani, and L. Boulon, "Towards health-aware energy management strategies in fuel cell hybrid electric vehicles: A review," *International Journal of Hydrogen Energy*, vol. 47, no. 17, pp. 10021–10043, Feb. 2022, doi: 10.1016/j.ijhydene.2022.01.064.
- [14] X. Lu and H. Wang, "Optimal sizing and energy management for cost-effective PEV hybrid energy storage systems," *IEEE Transactions on Industrial Informatics*, vol. 16, no. 5, pp. 3407–3416, May 2020, doi: 10.1109/TII.2019.2957297.
- [15] S.-Y. Chen, C.-Y. Chiu, Y.-H. Hung, K.-K. Jen, G.-H. You, and P.-L. Shih, "An optimal sizing design approach of hybrid energy sources for various electric vehicles," *Applied Sciences*, vol. 12, no. 6, Mar. 2022, doi: 10.3390/app12062961.
- [16] I.-S. Sorlei *et al.*, "Fuel cell electric vehicles-a brief review of current topologies and energy management strategies," *Energies*, vol. 14, no. 1, Jan. 2021, doi: 10.3390/en14010252.
- [17] H. Çınar and I. Kandemir, "Active energy management based on meta-heuristic algorithms of fuel cell/battery/supercapacitor energy storage system for aircraft," *Aerospace*, vol. 8, no. 3, Mar. 2021, doi: 10.3390/aerospace8030085.
- [18] D. Rimpas *et al.*, "Energy management and storage systems on electric vehicles: A comprehensive review," *Materials Today: Proceedings*, vol. 61, pp. 813–819, 2022, doi: 10.1016/j.matpr.2021.08.352.
- [19] W. Wu, J. S. Partridge, and R. W. G. Bucknall, "Simulation of a stabilised control strategy for PEM fuel cell and supercapacitor hybrid propulsion system for a city bus," *International Journal of Hydrogen Energy*, vol. 43, no. 42, pp. 19763–19777, Oct. 2018, doi: 10.1016/j.ijhydene.2018.09.004.
- [20] K. Wang, W. Wang, L. Wang, and L. Li, "An improved SOC control strategy for electric vehicle hybrid energy storage systems," *Energies*, vol. 13, no. 20, Oct. 2020, doi: 10.3390/en13205297.
- [21] R. S. Sankarkumar and R. Natarajan, "Energy management techniques and topologies suitable for hybrid energy storage system powered electric vehicles: An overview," *International Transactions on Electrical Energy Systems*, vol. 31, no. 4, Apr. 2021, doi: 10.1002/2050-7038.12819.
- [22] Z. Cabrane, D. Batool, J. Kim, and K. Yoo, "Design and simulation studies of battery-supercapacitor hybrid energy storage system for improved performances of traction system of solar vehicle," *Journal of Energy Storage*, vol. 32, Dec. 2020, doi: 10.1016/j.est.2020.101943.
- [23] B. Bendjedja, N. Rizoug, M. Boukhniher, and F. Bouchafaa, "Improved energy management strategy for a hybrid fuel cell/battery system," *COMPEL-The international journal for computation and mathematics in electrical and electronic engineering*, vol. 36, no. 4, pp. 1008–1027, Jul. 2017, doi: 10.1108/COMPEL-08-2016-0336.
- [24] W. Jiang *et al.*, "Control of the distributed hybrid energy storage system considering the equivalent SOC," *Frontiers in Energy Research*, vol. 9, Sep. 2021, doi: 10.3389/fenrg.2021.722606.
- [25] T. Sadeq, C. K. Wai, and E. Morris, "Current control of battery-supercapacitors system for electric vehicles based on rule-based linear quadratic regulator," *Advances in Science, Technology and Engineering Systems Journal*, vol. 6, no. 1, pp. 57–65, Jan. 2021, doi: 10.25046/aj060107.
- [26] H. Jbari, R. Askour, and B. B. Idrissi, "Fuzzy logic-based energy management strategy on dual-source hybridization for a pure electric vehicle," *International Journal of Electrical and Computer Engineering (IJECE)*, vol. 12, no. 5, pp. 4903–4914, Oct. 2022, doi: 10.11591/ijece.v12i5.pp4903-4914.

- [27] T. Hu, Y. Li, Z. Zhang, Y. Zhao, and D. Liu, "Energy management strategy of hybrid energy storage system based on road slope information," *Energies*, vol. 14, no. 9, Apr. 2021, doi: 10.3390/en14092358.
- [28] G. Xiao, Q. Chen, P. Xiao, L. Zhang, and Q. Rong, "Multiobjective optimization for a li-ion battery and supercapacitor hybrid energy storage electric vehicle," *Energies*, vol. 15, no. 8, Apr. 2022, doi: 10.3390/en15082821.
- [29] Amin, R. T. Bambang, A. S. Rohman, C. J. Dronkers, R. Ortega, and A. Sasongko, "Energy management of fuel cell/battery/supercapacitor hybrid power sources using model predictive control," *IEEE Transactions on Industrial Informatics*, vol. 10, no. 4, pp. 1992–2002, Nov. 2014, doi: 10.1109/TII.2014.2333873.
- [30] M. A. Zdiri *et al.*, "Design and analysis of sliding-mode artificial neural network control strategy for hybrid PV-battery-supercapacitor system," *Energies*, vol. 15, no. 11, Jun. 2022, doi: 10.3390/en15114099.
- [31] M. Gaber, S. El-Banna, M. El-Dabah, and O. Hamad, "Designing and implementation of an intelligent energy management system for electric ship power system based on adaptive neuro-fuzzy inference system (ANFIS)," *Advances in Science, Technology and Engineering Systems Journal*, vol. 6, no. 2, pp. 195–203, Mar. 2021, doi: 10.25046/aj060223.
- [32] W. Yaici, L. Kouchachvili, E. Entchev, and M. Longo, "Dynamic simulation of battery/supercapacitor hybrid energy storage system for the electric vehicles," in *2019 8th International Conference on Renewable Energy Research and Applications (ICRERA)*, Nov. 2019, pp. 460–465, doi: 10.1109/ICRERA47325.2019.8996509.
- [33] K. Ye, P. Li, and H. Li, "Optimization of hybrid energy storage system control strategy for pure electric vehicle based on typical driving cycle," *Mathematical Problems in Engineering*, pp. 1–12, Jun. 2020, doi: 10.1155/2020/1365195.
- [34] M. Haidoury and M. Rachidi, "Dynamic fuel cell model improvement based on macroscopic energy representation," *International Journal of Power Electronics and Drive Systems (IJPEDS)*, vol. 13, no. 3, pp. 1430–1439, Sep. 2022, doi: 10.11591/ijpeds.v13.i3.pp1430-1439.
- [35] G. L. Lopez, R. S. Rodriguez, V. M. Alvarado, J. F. Gomez-Aguilar, J. E. Mota, and C. Sandoval, "Hybrid PEMFC-supercapacitor system: Modeling and energy management in energetic macroscopic representation," *Applied Energy*, vol. 205, pp. 1478–1494, Nov. 2017, doi: 10.1016/j.apenergy.2017.08.063.
- [36] T. X. Dinh *et al.*, "Modeling and energy management strategy in energetic macroscopic representation for a fuel cell hybrid electric vehicle," *Journal of Drive and Control*, vol. 16, no. 2, pp. 80–90, 2019.
- [37] S. Elert, "Programming possibilities using MATLAB Simulink embedded Coder on the example of data analysis from ahrs module," *Journal of Physics: Conference Series*, vol. 1507, no. 8, Mar. 2020, doi: 10.1088/1742-6596/1507/8/082042.
- [38] C. Venugopal and T. Govender, "Load power and energy management system using proteus visual design software," *Indonesian Journal of Electrical Engineering and Computer Science (IJECS)*, vol. 20, no. 2, Nov. 2020, doi: 10.11591/ijeecs.v20.i2.pp1044-1052.
- [39] A. Chalh, A. El Hammoumi, S. Motahhir, A. El Ghzizal, U. Subramaniam, and A. Derouich, "Trusted simulation using proteus model for a PV system: test case of an improved HC MPPT algorithm," *Energies*, vol. 13, no. 8, Apr. 2020, doi: 10.3390/en13081943.
- [40] T. Wilberforce, M. Biswas, and A. Omran, "Power and voltage modelling of a proton-exchange membrane fuel cell using artificial neural networks," *Energies*, vol. 15, no. 15, Aug. 2022, doi: 10.3390/en15155587.
- [41] S. Ghosh, A. Routh, M. Rahaman, and A. Ghosh, "Modeling and control of a PEM fuel cell performance using artificial neural networks to maximize the real time efficiency," in *2019 International Conference on Energy Management for Green Environment (UEMGREEN)*, Sep. 2019, pp. 1–4, doi: 10.1109/UEMGREEN46813.2019.9221428.
- [42] F. Z. Belhaj, H. El Fadil, Z. El Idrissi, A. Intidam, M. Koundi, and F. Giri, "New equivalent electrical model of a fuel cell and comparative study of several existing models with experimental data from the PEMFC Nexa 1200 W," *Micromachines*, vol. 12, no. 9, Aug. 2021, doi: 10.3390/mi12091047.
- [43] C. Restrepo, T. Konjedic, A. Garces, J. Calvente, and R. Giral, "Identification of a proton-exchange membrane fuel cell's model parameters by means of an evolution strategy," *IEEE Transactions on Industrial Informatics*, vol. 11, no. 2, pp. 548–559, Apr. 2015, doi: 10.1109/TII.2014.2317982.
- [44] L. Zhang, X. Hu, Z. Wang, F. Sun, and D. G. Dorrell, "A review of supercapacitor modeling, estimation, and applications: A control/management perspective," *Renewable and Sustainable Energy Reviews*, vol. 81, pp. 1868–1878, Jan. 2018, doi: 10.1016/j.rser.2017.05.283.
- [45] Z. Cabrane and S. H. Lee, "Electrical and mathematical modeling of supercapacitors: comparison," *Energies*, vol. 15, no. 3, Jan. 2022, doi: 10.3390/en15030693.
- [46] M. Haidoury, H. Jbari, and M. Rachidi, "Modeling and control of fuel cell/supercapacitor hybrid source based on energetic macroscopic representation," *E3S Web of Conferences*, vol. 297, Sep. 2021, doi: 10.1051/e3sconf/202129701049.
- [47] S. Kavyapriya and R. K. Kumar, "Modeling and simulation of DC DC converters for fuel cell system," *International Journal of Engineering and Advanced Technology*, vol. 9, no. 3, pp. 2495–2500, Feb. 2020, doi: 10.35940/ijeat.C5754.029320.
- [48] K. Bharathi and M. Sasikumar, "Power flow control based on bidirectional converter for hybrid power generation system using microcontroller," *Microprocessors and Microsystems*, vol. 82, Apr. 2021, doi: 10.1016/j.micpro.2021.103950.

BIOGRAPHIES OF AUTHORS



Mohamed Haidoury    was born in Chefchaouen, Morocco in 1985. He received an engineer's degree in electromechanics from the National School of Arts and Crafts, (ENSAM-Meknes) in 2012. He obtained the master's degree in science and technology, specializing in science and information systems from ENSAM Paris-tech center Aix-en-Provence in French, in 2013. Currently, he is pursuing the Ph.D. with the National School of Arts and Crafts (ENSAM-Meknes), in the laboratory modeling, information processing and control systems (MTICS), Meknes, Morocco. His research focuses on the modeling and control of a multi-source system. Application to the traction of electric vehicles. He can be contacted at email: haidoury.mohamed@gmail.com.



Mohammed Rachidi    was born in Bejaad, Morocco. He received the engineer's degree from Mohammadia School of Engineers (EMI-Rabat), Morocco, in 1995 and the Ph.D. degree from National School of Arts and Crafts (ENSAM-Meknes), Moulay Ismail University, Meknes, Morocco, in 2017. His search interest is power electronics and control of electrical machines. Since 1997, he has been working at National School of Arts and Crafts (ENSAM-Meknes), Moulay Ismail University, Meknes, Morocco, where he is a professor in the Department of Electromechanical Engineering. He can be contacted at email: morachidi@yahoo.fr.



Hicham El hadraoui    was born in Rhamna, Morocco. He received the engineer's degree from Higher Normal School of Technical Education of Mohammedia (ENSET-M), Morocco, in 2017. He is a Ph.D. Student researcher at Green Tech Institute (GTI)/Mohammed VI Polytechnic University (UM6P), BenGuerir, Morocco, and had an experience as a Consulting Engineer in the automotive sector. His research interest is E-Mobility, especially control and diagnostic of the electric powertrain using artificial intelligent technics. He can be contacted at email: elhadraoui.hi@gmail.com.



Oussam Laayati    was born in Safi, Morocco. He received the engineer's degree from Higher Normal School of Technical Education of Mohammedia (ENSET-M), Morocco, in 2017. He is a Ph.D. Student researcher at Green Tech Institute (GTI)/Mohammed VI Polytechnic University (UM6P), BenGuerir, Morocco, working on smart grid energy automation, predictive maintenance, and digital twin projects. Experienced in modelling and designing electrical systems, renewable energies, PLC, DCS, SCADA systems integrating data analytics and machine learning features for prediction and optimization solutions. He can be contacted at email: Oussama.laayati@gmail.com.



Zakaria Kourab    was born in Casablanca, Morocco in 1987. He received an engineer's degree in electromechanics from the National High School of Arts and Crafts, (ENSAM-Meknes) in 2012. Currently, he is pursuing the Ph.D. with the National High School of Arts and Crafts (ENSAM-Casablanca), in the laboratory Complex Cyber Physical Systems (CCPS), Casablanca, Morocco. His research focuses on energy management systems, modeling and control of multi-source system. He can be contacted at email: zakaria.kourab@gmail.com.



Souad Tayane    is a professor of industrial chemistry at ENSAM Casablanca, specializing in research on smart, bio-based and biomaterials materials. She obtained her HDR in Industrial Chemistry at Hassan II University in Casablanca and was a researcher at Louis Pasteur University in Strasbourg. Tayane is also an ILO accredited trainer of trainers in entrepreneurship and project management. She has held editorial positions, chaired national and international workshops and is Secretary General of the Moroccan Association of Green and Alternative Energies (AMEVA). She can be contacted at email: souadtayane2013@gmail.com.



Mohamed Ennaji    was born in Casablanca, Morocco in 1983. He received the master's degree in industrial systems engineering aeronautical option from the Évry Val-d'Essonne University, (Évry-Courcouronnes) in 2008. Also, he earned his Ph.D. in Electrical Engineering, specializing in Wind turbine modeling at ENSEM in 2015. He is also a Professor of Mechatronics, Computer-Aided Design, and Manufacturing. He is head of the Rapid Prototyping Laboratory at the National School of Arts and Crafts of Casablanca. He is involved in various research projects, on topics such as new actuator technologies, new rapid prototyping processes, programmable matter, exoskeletons and Unmanned Aerial Vehicles. he is also a senior research engineer in aeronautics, robotics and biomedical projects, with the Mohammed VI Polytechnic University. He can be contacted at email: ennaji.moh@gmail.com.